# Crystal dislocations as a probe of electron topology in topological insulators

Shannon Egan
*Department of Physics and Astronomy, University of British Columbia, Vancouver, B.C., V6T 1Z1, Canada*
(Dated: December 20, 2020)

Topological materials have garnered much attention for their gapless surface states, which are robust against perturbations like disorder, thermal fluctuations and crystal defects. These properties make them attractive for future quantum devices, especially those that require storing information with high fidelity or carrying current with minimal loss. We can think of these surface states as mediating the transition between the nontrivial topology of the crystal interior, and the trivial topology of the surrounding vacuum. It turns out that some crystal defects also provide an interface on which these "topologically protected" gapless states can form. A particularly interesting example is dislocations, a 1D defect characterized by an abrupt change in crystal structure across a straight line. This report will explore the phenomenon of dislocations in topological insulators, with special focus on how gapless states bound to dislocation lines can be used to determine the material's topological phase. These ideas open the door to characterizing topological materials by probing properties of the bulk, rather than the boundary.

## I. PRELIMINARIES

### A. Topological insulators and their surface states

A universal feature of topological materials is the bulk-boundary correspondence, whereby the nontrivial topology of the bulk gives rise to electronic surface states localized to the edges of the material [1, 2]. A common mechanism of generating a band structure with nontrivial topology is called band inversion, which is illustrated in Figure 1. In a strong topological insulator (TI), the bulk band-structure is gapped, but the bands have an *odd* number of inversions relative to a trivial insulating state. The signature of this topological phase is electronic surface states which reside within the band gap, and which connect the filled valence band to the empty conduction band. These $d-1$ dimensional surface states are therefore conducting, even though the $d$ dimensional interior is insulating.

An intersecting pair of surface states is is called a Dirac cone, since the bands disperse linearly in the vicinity of the crossing point and therefore can be described by a relativistic Dirac Hamiltonian (see e.g. [3]).

$$H_D = \sum_{a=1}^{3} k_a \gamma_a + m\gamma_4 \tag{1}$$

Where $\mathbf{k}$ is the momentum very close to the crossing point, and the $\gamma_a$ are the 4-by-4 gamma matrices, which typically act in a Hilbert space of 2 orbitals and 2 spins, and $m$ is the mass of the relevant quasiparticle.

The topological phase of a 3D TI is described by four $\mathbb{Z}_2$ invariants $(\nu_0; \nu_1, \nu_2, \nu_3)$ which take a value of either 0 or 1 [4].

Strong TIs ($\nu_0 = 1$) have very robust surface states protected by time reversal symmetry (TRS) and the bulk band gap. This protection means that we can vary the Hamiltonian parameters, and even add new terms, but the surface states will remain gapless and present at the same $\mathbf{k}$-point as long as TRS is not broken, and the gap between valence and conduction bands never closes in the process. On the other hand, if we vary the parameters in a way that closes and reopens the bulk gap while respecting TRS, then we may enter a distinct topological phase.

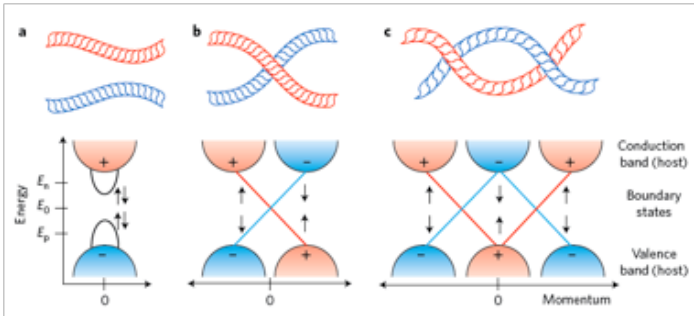


FIG. 1. Schematic of the evolving topology of a band structure through a series of band inversions. Each panel represents a distinct topological phase which cannot be smoothly deformed into the other two.

The set of topological phases in 3D TIs is spanned by the three "weak invariants" $\nu_1, \nu_2, \nu_3$. We can use these to construct a 3D vector which will be useful in characterizing dislocations:

$$\mathbf{M}_\nu \equiv \frac{1}{2}(\nu_1 \mathbf{G}_1 + \nu_2 \mathbf{G}_2 + \nu_3 \mathbf{G}_3) \tag{2}$$

where the $\mathbf{G}_i$ are reciprocal lattice vectors in momentum space. Weak TIs ($\nu_0 = 0$ but $\mathbf{M}_\nu \neq 0$) will only exhibit boundary states on surfaces that are *not* orthogonal to $\mathbf{M}_\nu$ [5]. For details on calculation of the $\mathbb{Z}_2$ invariants, we refer the reader to early papers by Fu and Kane [4, 6],

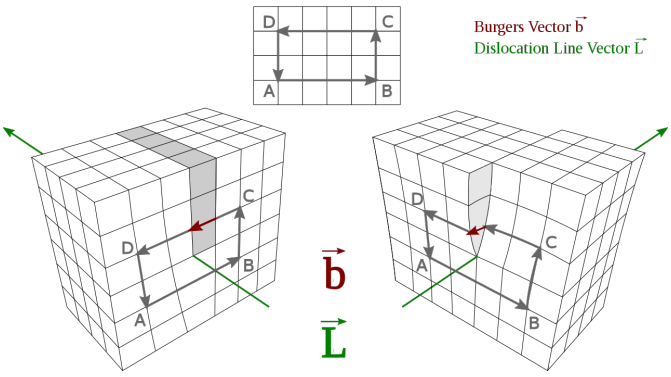


FIG. 2. Schematic of a square 3D lattice with edge (left) and screw (right) dislocation. The grey loop ABCD can be used to determine the Burgers vector as follows: On the defect-free lattice, draw the directed loop such that it encloses the dislocation and defines a plane perpendicular to **L**. Then, distort the lattice by displacing all atoms in one quadrant (in this case, the upper right) by one lattice vector **a** with either $\mathbf{a} \perp \mathbf{L}$ (edge) or $\mathbf{a} \parallel \mathbf{L}$ (screw). The Burger's vector is exactly the extra portion of the loop which was not present before the distortion.

or to relevant textbooks and reviews [1, 2].

### B. Dislocations

Dislocations are line defects which often form during crystal growth. The two main varieties are edge and screw dislocations. The former occur when a plane of atoms terminates in the middle of the crystal, such that the layers on either side must grow around it; the latter will be discussed in Section II A. We define dislocations mathematically by two vectors:

1. Tangent vector **L**, which points along the dislocation line.
2. Burgers vector **b**, which describes the distortion of the lattice around the dislocation. It must be a lattice vector.

We can determine the Burgers vector using the construction illustrated in Figure 2. The crystal ordering is only disrupted very close to the dislocation line, and the regular lattice is restored at large radial distances. Does this mean that dislocations only affect electron behaviour locally?

To answer this, consider the directed loop ABCD drawn in Figure 2. Whether we make the loop smaller or extend it to infinity, we will always find the same Burgers vector. The fact that the Burgers vector, which defines the dislocation, is invariant with respect to deformations of the loop is what makes dislocations "topological defects" [7].

In contrast, other types of crystal defects such as vacancies or replacements are purely local. They distort the lattice only in a small range and cannot be detected from far away. We don't expect local defects to impact the long-range behaviour of electrons. However, the fact that a dislocation can be detected nonlocally suggests that they may have an impact on global electron behaviour.

## II. DISLOCATIONS AS A PROBE OF TOPOLOGY

Ran et al. showed in reference [8] that there is a deep, yet simple, connection between the weak $\mathbb{Z}_2$ topological invariants and the existence of gapless states on crystal dislocations. Namely if the dot product $\mathbf{b} \cdot \mathbf{M}_\nu$ is an odd multiple of $\pi$, i.e.

$$\mathbf{b} \cdot \mathbf{M}_\nu = \pi (\mathrm{mod}\, 2\pi) \tag{3}$$

then the dislocation hosts 1D gapless edge modes protected by TRS and the bulk band gap. Because the system obeys TRS, these dislocation modes must appear as pairs with opposite spins propagating in opposite directions, and thus resemble the chiral edge states of a 2D Quantum Spin Hall (QSH) insulator [9, 10].

We can see immediately how the dislocation could help us to distinguish different phases. First of all, if $\nu_1 = \nu_2 = \nu_3 = 0$ then we will not find dislocation modes for any **b**. However, if any of the weak indices are non-zero, then we may be able to satisfy the condition for some magnitude and direction of **b**, but not for others. Experimentally, we could detect dislocation modes by measuring the density of states (DOS) at the surface of the material (e.g. using scanning tunnelling microscopy). The signature of the modes is a peak in the DOS at the point where the dislocation line reaches the surface. A simulated measurement of this character is shown in Figure 5 c.

To better understand the physical origins of Equation 3, we will analyze an example of a tight-binding model with a screw dislocation in Section II A. In Section II B, we review other approaches to dislocations in TIs to elucidate the rich range of related phenomena.

### A. Screw dislocation in a distorted diamond-lattice

This section follows the derivation of Ran et al. [8] to demonstrate that a screw dislocation in a tight-binding (TB) model of a TI indeed has edge modes that propagate along the dislocation line, but only if Equation 3 is satisfied.

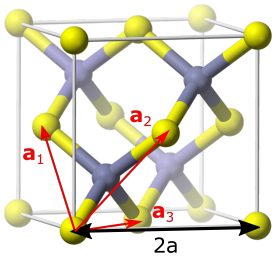


FIG. 3. Diagram of the diamond lattice with cubic unit cell of size $2a$. $a_i$ are the three lattice vectors when the unit cell is defined with a two atom basis (yellow and grey spheres). $a_3$ is the direction of the dislocation in Section II A.

We begin with a TB model of a diamond lattice with nearest-neighbour (n.n.) hopping and spin-orbit coupling (SOC).

$$H = t\sum_{\langle ij\rangle} c^\dagger_{i\sigma}c_{j\sigma} + i\frac{\lambda_{SO}}{(2a)^2}\sum_{\langle\langle ij\rangle\rangle} c^\dagger_{i\sigma}\left(\mathbf{d}^1_{ij}\times\mathbf{d}^2_{ij}\right)\cdot\boldsymbol{\sigma}_{\sigma\sigma'}c_{j\sigma'} \tag{4}$$

where $c_{i\sigma}$ is the annihilation operator for an electron with spin $\sigma$ at site $i$, $t$ is the hopping amplitude, $\lambda_{SO}$ is the SOC amplitude, $\mathbf{d}^1_{ij}$,$\mathbf{d}^2_{ij}$ are vectors tracing the two n.n. bonds between $i$ and the next-to-nearest neighbour site $j$, $\boldsymbol{\sigma}$ is a vector containing the three Pauli matrices (with $\boldsymbol{\sigma}_{\sigma\sigma'}$ denoting a particular component), and finally $2a$ is the cubic unit cell size.

This model as written is a trivial insulator, but if we distort the lattice so that $t \to t + \delta t$ along the $\frac{a}{2}(1,1,1)$ direction, then the system becomes a strong TI for $\delta t > 0$, and a weak TI for $\delta t < 0$ with $\mathbf{M}_\nu = \frac{\pi}{2a}(1,1,1)$ [4].

We now insert a screw dislocation along the $\mathbf{a}_3 = a(1,1,0)$ direction (See Figure 3). To do so, we cut all bonds intersecting the "slip plane" $P$, pictured in Figure 4, which is orthogonal to $(1,-1,-1)$ and terminates at the dislocation. We then shift all atoms above $P$ by the length of the Burgers vector $\mathbf{b} = \mathbf{a}_3$. We can model the "slip" across the dislocation by adding a phase to the hopping parameter $t \to te^{ik\,\hat{k}\cdot\mathbf{b}}$ for all bonds intersecting $P$.

If momentarily we set the hopping across this plane to zero, then we have two decoupled surfaces denoted $S_+$ and $S_-$. Since the 3D material is a TI, we know that each surface hosts an odd number of Dirac cones. For this model on the (1,-1,-1) surface, there is a single Dirac cone at surface momentum $\mathbf{m}_D = \frac{\pi}{2a}(1,1,0)$. This allows us to write an effective Hamiltonian $\pm H_0$ similar to Equation 1 for the surfaces $S_\pm$, since the Dirac cones will dominate the low-energy physics:

$$H_0(p) = \nu_1 p_1\hat{n}_1\cdot\boldsymbol{\sigma} + \nu_2 p_2\hat{n}_2\cdot\boldsymbol{\sigma} \tag{5}$$

where the $p_i$ are surface momenta measured from the Dirac point $\mathbf{m}_D$. $\hat{n}_1$ and $\hat{n}_2$ are orthogonal unit vectors

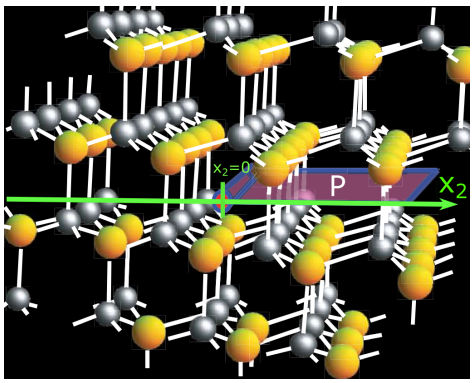


FIG. 4. Diamond lattice with slip plane $P$ terminating at the dislocation. Bonds intersecting $P$ are cut, then shifted along the dislocation by Burgers vector $\mathbf{b}$ to form a screw dislocation. The $x_2$ axis is orthogonal to the dislocation line, which is located at $x_2 = 0$. Figure adapted from [8].

defining $P$, where $p_1\hat{n}_1$ is the momentum along the dislocation line. The $\nu_1$, $\nu_2$ are the usual weak topological invariants.

Now let's add an effective coupling $m$ between the two surfaces. We introduce the Pauli matrices $\tau_i$ which act in the Hilbert space of the $S_\pm$ surface states, and take tensor products with $H_0(p)$. The effective Hamiltonian becomes:

$$H_{eff} = H_0(p)\otimes\tau_z + m(\mathbb{1}_{2\times2}\otimes\tau_x) \tag{6}$$

where the coupling $m$ opens a gap, making it topologically equivalent to the bulk insulator. The Dirac quasiparticles on $S_\pm$ pick up a phase difference as they hop across the slip plane, such that $m \to e^{i\phi}m$. Since the Dirac node is at $\mathbf{m}_D$, the phase is:

$$\phi = \mathbf{m}_D\cdot\mathbf{b} = \pi \tag{7}$$

Using the coordinates defined in Figure 4, we write the effective Hamiltonian with dislocation as (with tensor product symbols dropped for brevity):

$$H_{\text{dis}} = H_0(-i\hbar\nabla)\tau_z + \begin{cases} m\tau_x & x_2 < 0 \\ -m\tau_x & x_2 > 0 \end{cases} \tag{8}$$

Where we have set $p \to -i\hbar\nabla$ due to the disruption of translational invariance in the $p_2$ direction. $p_1$ is still a good quantum number since it is along the dislocation.

It is crucial that $\mathbf{b}\cdot\mathbf{m}_D$ is not an integer multiple of $2\pi$, which would result in a trivial phase. Instead, the phase causes a change in the effective Hamiltonian when we cross from the "unslipped" region ($x_2 < 0$) to the "slipped" region ($x_2 > 0$) after the dislocation.

The final step is to show that this Hamiltonian admits gapless states, and that they are localized to the

dislocation line at $x_2 = 0$. This is simplest to solve by setting $p_1 = 0$, such that:

$$H_{\text{dis}}(p_1 = 0) = \nu_2 \hat{n}_2 \cdot \boldsymbol{\sigma} \tau_z (-i\hbar\partial_{x_2}) + m_2(x_2)\tau_x \quad (9)$$

As shown by Jackiw and Rossi, this type of Hamiltonian has a pair of zero-energy solutions given by:

$$\psi(x_2) = e^{\frac{1}{\hbar\nu_2}\int_0^{x_2} dx_2 m(x_2)}\psi_0 \quad (10)$$

where $\psi_0$ is an eigenstate of $\tau_y \hat{n}_2 \cdot \boldsymbol{\sigma}$ [11].

Thanks to the nontrivial phase difference $e^{i\mathbf{m}_D \cdot \mathbf{b}} = -1$, the solution is a decaying exponential on both sides of $x_2 = 0$. From this we can conclude that the state is localized to the dislocation line.

The numerical results in Figure 5 confirm that the dislocation modes have a linear dispersion about the Dirac point in k-space, and that they connect the gapped valence and conduction bands. Therefore they satisfy the qualities we expect for the surface states of a 2D TI arising due to the bulk-boundary correspondence.

As a closing remark for this section, we connect the results back to the general existence condition in Equation 3. Recall that $\mathbf{M}_\nu = \frac{\pi}{2a}(1,1,1)$. Since the Burgers vector had no z-component, it is clear that:

$$\mathbf{b} \cdot \mathbf{M}_\nu = \mathbf{b} \cdot \mathbf{m}_D = \pi \quad (11)$$

which shows that our our effective Hamiltonian approach was consistent with the general condition's prediction.

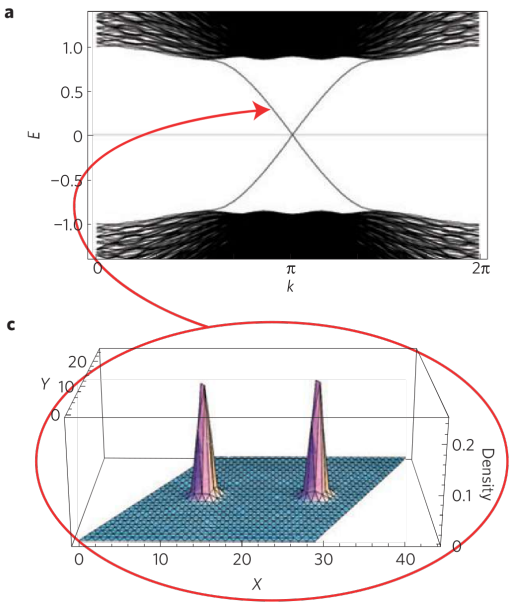


FIG. 5. Numerical simulation of a screw dislocation in the diamond-lattice strong topological insulator. The Burgers vector $\mathbf{b}$ is parallel to the lattice direction $\mathbf{a}_3$ and points along the dislocation line. Panel **a** shows the energy spectrum with two pairs of counterpropagating gapless 1D modes, one for each disloaction, which disperse linearly around the crossing and connect the valence bands to the conduction bands. $k$ is the momentum along the dislocation. Panel **c** shows the simulated density of states at the surface, with two clear peaks corresponding to the $(x, y)$ position of each dislocation.

### B. Other approaches to dislocations in TIs

Equation 3 provides an elegant and fully general existence condition for dislocation modes in TIs, but it does not teach us much about the physics of these dislocations. Here we review a few different approaches to modelling dislocations which provide alternative perspectives on why these dislocation modes arise.

#### 1. *Stress tensor approach to the lattice distortion*

So far we have described TIs whose robust surface states are protected by TRS alone. However, there exist other classes of TIs whose surface states are protected instead by crystal symmetries, i.e. they are protected by the geometry of the lattice itself. When a topological phase requires the combination of TRS and crystal symmetries to protect the surface states, the Dirac cones appear at edges of the Brillouin zone (BZ) and the phase is called "translationally-active" [12].

Slager et al. show that dislocations distinguish the translationally active phase from the stronger "Γ phase" (protected only by TRS) in 2D, as dislocation modes appear only in the former phase [13]. They approach the problem using "elastic continuum theory" to describe the lattice distortions generated by the dislocation. This strategy relies on the fact that local crystal order is only disrupted very close to the dislocation. We can thus approximate the microscopic region around the dislocation line as a continuum, and use tensors to describe the distortion field of the crystal in this region.

Like the previous section, we can assume that the low energy physics is dominated by the surface Dirac cones, and consider only momenta in a small radius around the Dirac point $\mathbf{K}_{inv}$ [1]. The momentum is modified by the presence of the dislocation as follows:

$$k_i = (\mathbf{e}_i + \boldsymbol{\varepsilon}_i) \cdot (\mathbf{K}_{inv} - \mathbf{q}) \quad (12)$$

where $\mathbf{e}_i$ are the Cartesian coordinate unit vectors and $\varepsilon_i$ is the distortion field of the dislocation. We can thus

[1] We label it with the subscript *inv* for inversion, because a band inversion occurs at the Dirac point.

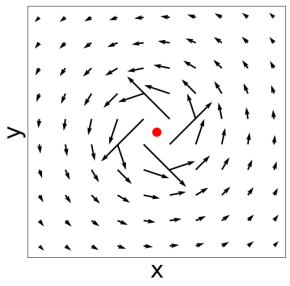


FIG. 6. Vector field representing the effective gauge field in Equation 13. The red point represents the dislocation centre.

treat the dislocation as inducing a gauge field $A_i = \varepsilon_i$, such that $\mathbf{q} \to \mathbf{q} + \mathbf{A}$. For an edge dislocation in 2D, the gauge field is:

$$\mathbf{A}_{2D} = \frac{-y\mathbf{e}_x + x\mathbf{e}_y}{2r^2} \tag{13}$$

which circulates counter-clockwise around the dislocation at $r = 0$, and decays quickly away from it (See Figure 6). This gauge field is analogous to the vector potential of an infinite solenoid localized at the dislocation center. Thus we can think of the dislocation as creating a magnetic defect called a $\pi$-flux within the lattice. The existence of this $\pi$-flux has two main implications: 1) electrons travelling in a circle around the dislocation will acquire a phase, just like to the Aharonov-Bohm effect and 2) that the dislocation can host zero-energy bound states [14].

In 3D the effective gauge field of the dislocation (both edge and screw) is similar, but modified by a flux $\Phi = \mathbf{K}_{inv} \cdot \mathbf{b}$

$$\mathbf{A}_{3D} = \frac{-y\mathbf{e}_x + x\mathbf{e}_y}{2\pi r^2}\Phi \tag{14}$$

where $\mathbf{K}_{inv}$ must be in the plane perpendicular to the dislocation direction $\mathbf{L}$, i.e. a Dirac cone exists in this plane. The dislocation can only host bound states provided that $\Phi = \mathbf{K}_{inv} \cdot \mathbf{b} = \pi(\mathrm{mod}2\pi)$ [15]. So we have once again arrived at Equation 3, but by a very different route!

#### 2. *Topological invariants for defects*

Another approach to characterizing dislocation modes is inspired by the 10-fold way, an exhaustive classification scheme for topological insulators and superconductors [16, 17]. The 10-fold way tells us what kind of topological invariant ($\mathbb{Z}_2$, $\mathbb{Z}$ or the strictly trivial 0) can be used for a Hamiltonian of a certain symmetry class, depending on the presence or absence of TR and particle-hole symmetry, as well as their combination: chiral-symmetry.

Teo and Kane develop a similar classification scheme for topological line and point defects [18]. They define a parameter $\delta = d - D$, where $d$ is the dimension of the system and $D$ is the dimension of a surface enclosing the defect. Based only on the symmetry class and $\delta$, they can define a single topological invariant which will predict whether or not the topological defect will host gapless modes. They can also predict what kind of boundary mode will be present (e.g. Chiral Dirac fermion, chiral Majorana fermion, etc.). For line dislocations in a TI, they compute the $\mathbb{Z}_2$ topological defect invariant, and find that is only non-trivial when Equation 3 is also satisfied.

## III. DISCUSSION

Our survey of approaches to dislocations in TIs shows above all that the existence condition derived by Ran et al. is incredibly general. No matter the physical starting point, one can always re-derive Equation 3.

While studying this condition, we have seen that dislocations in TIs may be useful in experimental settings for diagnosing the topological phase of a material. Probing the bulk topological phase using dislocations is especially practical for weak TIs and topological crystalline insulators, where the surface states can be sensitive to disorder or to the direction that the surface is cleaved in [19]; and for higher order topological insulators (HOTIs), where the low dimensionality of the boundary states makes them difficult to detect [20].

More excitingly, dislocation modes may be good candidates for engineering quantum wires. The counter-propagating modes experience minimal backscattering due to their topological properties, leading to very efficient electrical transport.

A great obstacle to studying dislocation modes is the difficulty of controlling the density and direction of dislocations in a real crystal. This challenge stalled experimental realizations of Ran et al.'s theoretical proposal, but a recent paper suggests that the problems may be solvable. Using a rather crude method called plastic deformation to generate dislocations, Hamasaki et al. found that Bi-Sb crystals exhibited excess conductivity consistent with conduction through 1D dislocation modes [21]. If precise control on dislocation formation can be achieved, these structures could become a key-stepping stone towards novel quantum devices, including those necessary for topological quantum computing [22].

[1] X.-L. Qi and S.-C. Zhang, "Topological insulators and superconductors," *Reviews of Modern Physics*, vol. 83, no. 4, p. 1057–1110, Oct 2011. [Online]. Available: http://dx.doi.org/10.1103/RevModPhys.83.1057

[2] M. Franz and L. M. (Eds.), *Topological Insulators*, 1st ed., ser. Contemporary Concepts of Condensed Matter Science 6. Elsevier, 2013. [Online]. Available: http://gen.lib.rus.ec/book/index.php?md5=7111e2142c2f663e6ac2c328cb041d0a

[3] A. A. Burkov, M. D. Hook, and L. Balents, "Topological nodal semimetals," *Physical Review B*, vol. 84, no. 23, Dec 2011. [Online]. Available: http://dx.doi.org/10.1103/PhysRevB.84.235126

[4] L. Fu, C. L. Kane, and E. J. Mele, "Topological insulators in three dimensions," *Physical Review Letters*, vol. 98, no. 10, Mar 2007. [Online]. Available: http://dx.doi.org/10.1103/PhysRevLett.98.106803

[5] I. P. Rusinov, T. V. Menshchikova, A. Isaeva, S. V. Eremeev, Y. M. Koroteev, M. G. Vergniory, P. M. Echenique, and E. V. Chulkov, "Mirror-symmetry protected non-TRIM surface state in the weak topological insulator $Bi_2TeI$," *Scientific Reports*, vol. 6, p. 20734, Feb. 2016.

[6] L. Fu and C. L. Kane, "Topological insulators with inversion symmetry," *Phys. Rev. B*, vol. 76, p. 045302, Jul 2007. [Online]. Available: https://link.aps.org/doi/10.1103/PhysRevB.76.045302

[7] N. D. Mermin, "The topological theory of defects in ordered media," *Rev. Mod. Phys.*, vol. 51, pp. 591–648, Jul 1979. [Online]. Available: https://link.aps.org/doi/10.1103/RevModPhys.51.591

[8] Y. Ran, Y. Zhang, and A. Vishwanath, "One-dimensional topologically protected modes in topological insulators with lattice dislocations," *Nature Physics*, vol. 5, no. 4, pp. 298–303, Apr. 2009.

[9] C. L. Kane and E. J. Mele, "$Z_2$ topological order and the quantum spin hall effect," *Phys. Rev. Lett.*, vol. 95, p. 146802, Sep 2005. [Online]. Available: https://link.aps.org/doi/10.1103/PhysRevLett.95.146802

[10] A. Akhmerov, J. Sau, B. van Heck, S. Rubbert, and R. Skolasiński. Quantum spin hall effect. [Online]. Available: https://topocondmat.org/w5_qshe/fermion_parity_pump.html

[11] R. Jackiw and P. Rossi, "Zero modes of the vortex-fermion system," *Nuclear Physics B*, vol. 190, no. 4, pp. 681 – 691, 1981. [Online]. Available: http://www.sciencedirect.com/science/article/pii/0550321381900444

[12] R.-J. Slager, A. Mesaros, V. Juričić, and J. Zaanen, "The space group classification of topological band-insulators," *Nature Physics*, vol. 9, no. 2, pp. 98–102, Feb. 2013.

[13] V. Juričić, A. Mesaros, R.-J. Slager, and J. Zaanen, "Universal probes of two-dimensional topological insulators: Dislocation andflux," *Physical Review Letters*, vol. 108, no. 10, Mar 2012. [Online]. Available: http://dx.doi.org/10.1103/PhysRevLett.108.106403

[14] A. Mesaros, R.-J. Slager, J. Zaanen, and V. Juričić, "Zero-energy states bound to a magnetic -flux vortex in a two-dimensional topological insulator," *Nuclear Physics B*, vol. 867, no. 3, p. 977–991, Feb 2013. [Online]. Available: http://dx.doi.org/10.1016/j.nuclphysb.2012.10.022

[15] R.-J. Slager, A. Mesaros, V. Juričić, and J. Zaanen, "Interplay between electronic topology and crystal symmetry: Dislocation-line modes in topological band insulators," *Physical Review B*, vol. 90, no. 24, Dec 2014. [Online]. Available: http://dx.doi.org/10.1103/PhysRevB.90.241403

[16] A. P. Schnyder, S. Ryu, A. Furusaki, and A. W. W. Ludwig, "Classification of topological insulators and superconductors in three spatial dimensions," *Physical Review B*, vol. 78, no. 19, Nov 2008. [Online]. Available: http://dx.doi.org/10.1103/PhysRevB.78.195125

[17] A. P. Schnyder, S. Ryu, A. Furusaki, A. W. W. Ludwig, V. Lebedev, and M. Feigel'man, "Classification of topological insulators and superconductors," *AIP Conference Proceedings*, 2009. [Online]. Available: http://dx.doi.org/10.1063/1.3149481

[18] J. C. Y. Teo and C. L. Kane, "Topological defects and gapless modes in insulators and superconductors," *Phys. Rev. B*, vol. 82, p. 115120, Sep 2010. [Online]. Available: https://link.aps.org/doi/10.1103/PhysRevB.82.115120

[19] Z. Ringel, Y. E. Kraus, and A. Stern, "Strong side of weak topological insulators," *Physical Review B*, vol. 86, no. 4, Jul 2012. [Online]. Available: http://dx.doi.org/10.1103/PhysRevB.86.045102

[20] B. Roy and V. Juricic, "Dislocation as a bulk probe of higher-order topological insulators," 2020.

[21] H. Hamasaki, Y. Tokumoto, and K. Edagawa, "Conductive and non-conductive dislocations in bi–sb topological insulators," *Journal of the Physical Society of Japan*, vol. 89, no. 2, p. 023703, 2020. [Online]. Available: https://doi.org/10.7566/JPSJ.89.023703

[22] M. H. Freedman, A. Kitaev, M. J. Larsen, and Z. Wang, "Topological Quantum Computation," *arXiv e-prints*, pp. quant–ph/0 101 025, Jan. 2001.